

New Analogues of the BODIPY Dye PM597: Photophysical and Lasing Properties in Liquid Solutions and in Solid Polymeric Matrices

A. Costela,[†] I. García-Moreno,^{*,†} M. Pintado-Sierra,[†] F. Amat-Guerri,[‡] R. Sastre,[§] M. Liras,^{||} F. López Arbeloa,[⊥] J. Bañuelos Prieto,[⊥] and I. López Arbeloa[⊥]

Instituto de Química-Física Rocasolano, Serrano 119, 28006 Madrid, Spain, Instituto de Química Orgánica General, CSIC, Juan de la Cierva 3, 28006 Madrid, Spain, Instituto de Ciencia y Tecnología de Polímeros, Juan de la Cierva 3, 28006 Madrid, Spain, Universidad Miguel Hernández, Ferrocarril s/n, Edificio Torrevaillo, 03202 Elche, Alicante, Spain, and Departamento de Química-Física, UPV-EHU, Apartado 644, 48080 Bilbao, Spain

Received: March 26, 2009; Revised Manuscript Received: May 22, 2009

New tailor-made BODIPY dyes have been synthesized by a simple protocol to reach wavelength finely tunable laser action from 540 to 625 nm while maintaining highly efficient and photostable laser emission. The new dyes are analogues of the commercial dye PM597 with the eight position free (PTH8) or substituted by the groups acetoxymethyl (PTalk) or *p*-acetoxymethylphenyl (PTAr). The photophysical properties strongly depend on the geometrical distortion from planarity of the indacene core generated by the presence of the bulky 2,6-di-*tert*-butyl groups and the eight substituent. In both liquid and polymeric solid solutions, lasing efficiencies of up to 63 and 48%, respectively, were observed under transversal pumping at 532 nm with high photostabilities. In the case of PTalk incorporated into silicon-containing solid organic matrices, the laser emission remained at 92% of its initial intensity value after 100 000 pumping pulses in the same position of the sample at 30 Hz repetition rate. The laser action of the new dyes enhances that of the parent dye PM597 and outperforms the lasing behavior of dyes considered to be benchmarks over the green-yellow to red spectral region.

1. Introduction

Modern biotechnological, optical, and electronic applications require new fluorophores with predetermined properties such as high photostability, high fluorescence quantum yield, large Stokes shift, optimized absorption profile, and suitable anchoring groups so as to meet the demands for more sensitive analytical protocols, sensors, and light-emitting devices.^{1,2} 4,4-Difluoro-4-bora-3a,4a-diaza-*s*-indacene (BODIPY or BPD) dyes are currently some of the most used chromophores as active media for dye lasers because of their high lasing efficiency, low intersystem crossing probability, and good thermal, chemical, and photochemical stability.^{3–5} Several attempts have been made to shift the emission of BDPs over the visible spectral region, especially to the red, by substituting the chromophore core with an aryl group at the eight (or meso) position or with aryl, styryl, or ethynylphenyl groups at the 3,5-positions, or by introducing a nitrogen atom at the eight position (8-aza-BDPs), by fusing aromatic rings and so on, always trying to increase the delocalization of the electronic π -system.⁵ These chemical modifications can also induce new photophysical processes, such as photoinduced electron transfer, allowing the application of BDP dyes as molecular sensors in antenna systems or in light harvesting arrays.^{6–10}

To modulate to some extent the photophysical and lasing properties of BDP dyes by the introduction of appropriate

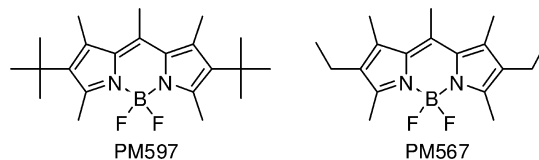


Figure 1. Structure of the laser dyes PM597 and PM567.

substitution patterns, over the last few years we have studied the effect of changing the 8-methyl group of the dye PM567 (Figure 1) by other groups while maintaining the rest of the substituents.¹¹ The presence of an acetoxymethyl or a methacryloyloxy group separated from the eight position by a polymethylene or a poly-*p*-phenylene chain does not significantly modify the photophysics of the chromophore, with regard to that of the parent dye PM567, especially if the linear polymethylene chain has five or more methylene groups.^{11b,d} The new dyes, when dissolved in a variety of organic solvents, lased more efficiently than PM567 and, under continuous UV irradiation, demonstrated improved photostability.^{11a,b} In addition, when these analogues of PM567 were either dissolved in poly(methyl methacrylate) (PMMA) or covalently bound to the same polymer, they lased more efficiently than the parent dye PM567 incorporated into PMMA.^{11c,d}

Looking for shifting this behavior to the red region of the spectrum, a number of analogues of 2,6-di-*tert*-butyl-1,3,5,7,8-pentamethyl-BDP, a laser dye commercially known as PM597 (Figure 1), have been synthesized following the above-described strategy. The fluorescence and lasing bands of PM597 are bathochromically shifted with respect to those of PM567.¹² Despite having a lower fluorescence quantum yield than PM567, PM597 exhibits high lasing efficiencies because its very high

* Corresponding author. E-mail: i.garcia-moreno@iqfr.csic.es. Tel: +34 91 5619400, ext. 1202. Fax: + 34 91 5642431.

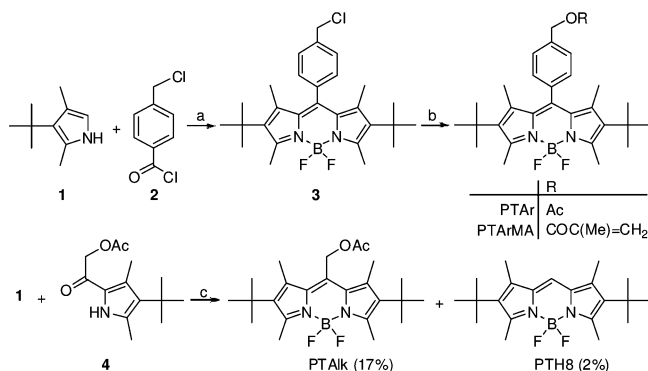
[†] Instituto de Química-Física Rocasolano.

[‡] Instituto de Química Orgánica General.

[§] Instituto de Ciencia y Tecnología de Polímeros.

^{||} Universidad Miguel Hernández.

[⊥] UPV-EHU.

SCHEME 1: Reagents and Conditions^a

^a (a) 1:2 molar ratio 2:1, CH_2Cl_2 , Ar, reflux, 5 h, then r.t., Et_3N , 30 min, then $\text{BF}_3 \cdot \text{OEt}_2$, 2 h, 23%; (b) PTAr: AcONa , Et_3N , DMF, Ar, 40 °C, 24 h, 23%; PTArMA: methacrylic acid, K_2CO_3 , Et_3N , DMF, Ar, 40 °C, 24 h, 20%; (c) 1:4 molar ratio 1:1, CH_2Cl_2 , Ar, r.t., 12 h, then Et_3N , 5 min, then $\text{BF}_3 \cdot \text{OEt}_2$, 1 h.

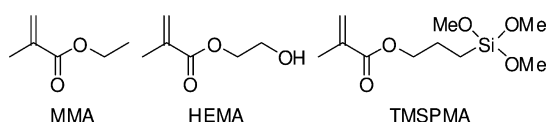


Figure 2. Structure of the monomers.

Stokes shift reduces the losses in the resonator cavity due to reabsorption/reemission phenomena.¹² Besides, PM597 is also characterized by its high photostability, rendering efficient laser signal after thousands of pumping pulses.¹³

In the present work, we have synthesized and characterized new BDP dyes with the same substituents as PM597 in positions one to seven but containing at position eight the groups *p*-acetoxymethylphenyl (PTAr), *p*-methacryloyloxymethylphenyl (PTArMA), hydrogen (PTH8), or acetoxymethyl (PTalk) (Scheme 1). PTAr is a model compound of the monomer PTArMA. PTArMA has been covalently bound to the polymeric chain of PMMA, rendering the solid copolymer COP(MMA-PTArMA). This copolymer provides additional channels for the dissipation of the excess absorbed energy; consequently, it was expected that the bound chromophore could show increased laser photostability.^{11c,d} The analogue PTH8 was also studied to gain deeper insight into the geometrical distortion from planarity of the substituted indacene core induced by the 2,6-di-*tert*-butyl and 1,7-dimethyl groups. The photophysical and lasing properties of the new analogues have been systematically analyzed in air-equilibrated liquid solutions in several solvents as well as in solid solutions of PMMA and in copolymers of MMA with 2-hydroxyethyl methacrylate (HEMA) or with the silylated monomer 3-(trimethoxysilyl)propyl methacrylate (TMSPMA) (Figure 2).^{11e,f}

2. Experimental Methods

2.1. Materials. The dyes PM597, PM567, and sulforhodamine B (all >99% purity, laser grade, from Exciton) were used as received; its purity was confirmed by spectroscopic and chromatographic methods. All commercial solvents used in photophysical and laser experiments were of the highest purity available and were used without further purification; those used in synthetic work were purified by standard methods. The monomer MMA (Merck) was successively washed with 5% aqueous NaOH and water, dried over Na_2SO_4 , and distilled under reduced pressure. HEMA (Aldrich) was distilled under reduced pressure before use. TMSPMA (Aldrich) was used as

received. Other reagents were from commercial sources and were used as received.

2.2. Preparation of Solid Polymeric Samples. Solid matrices of PMMA or of the copolymers of MMA with HEMA or with TMSPMA, incorporating PTAr, PTH8, PTalk, or PM597 as true solutions, and the solid copolymer of PTArMA with PMMA were prepared essentially as described elsewhere.^{11c} An adequate amount of the dye was dissolved in pure MMA or in its mixtures with HEMA or TMSPMA, and the resulting mixtures were polymerized by free radical bulk polymerization, yielding the materials named dye/PMMA, dye/COP(MMA-HEMA), dye/COP(MMA-TMSMA) (all true solutions), and COP(PTArMA-MMA) (dye copolymer). The solid samples were cast in a cylindrical shape, forming rods of 10 mm diameter and 10 mm length. A cut was made parallel to the axis of the cylinder to obtain a lateral flat surface of ca. 6×10 mm. We prepared this surface and the ends of the laser rods for lasing experiments by using a grinding and polishing machine (Phoenix Beta 4000, Büehler) until optical-grade finishing. The planar grinding stage was carried out with Texmet 1000 sand paper using as abrasive $6 \mu\text{m}$ diamonds suspended in mineral oil. The final polishing stage was made with a G-Tuch Microcloth, using a cloth disk Mastertex with $1 \mu\text{m}$ diamonds in mineral oil.

2.3. Photophysical Properties. The photophysical properties were registered in 2×10^{-6} M solutions in different solvents, prepared by adding the corresponding solvent to the residue from the adequate amount of a ca. 10^{-3} M stock solution in acetone after vacuum evaporation of the solvent. UV-vis absorption and fluorescence spectra were recorded on a Cary 4E spectrophotometer and on a SPEX Fluorolog 3-22 spectrofluorimeter, respectively. Fluorescence quantum yields (Φ_F) were evaluated from refractive-index-corrected spectra, using as a reference a 10^{-6} M solution of PM597 in methanol ($\Phi_F = 0.48$).¹² Radiative decay curves were registered with the time-correlated single-photon counting technique (Edinburgh Instruments, model FL920). Fluorescence emission was monitored at the maximum emission wavelength after excitation at 410 nm by means of a diode laser (PicoQuant LDH410) with 150 ps fwhm pulses, 10 MHz repetition rate, and a power supply of 0.65 mW. The fluorescence lifetime (τ) was obtained from the slope after the deconvolution of the instrumental response.

Quantum mechanical calculations were carried out in the Gaussian 03 software.¹⁴ Ground state (S_0) geometry was optimized with the B3LYP method, whereas the first excited singlet (S_1) geometry was obtained by means of the CIS method. In both cases, the double valence basis set was used. The spectral transitions were simulated with the time-dependent (TD-B3LYP) method: absorption via the Franck-Condon transition from S_0 and fluorescence via the vertical transition from S_1 .

2.4. Laser Evaluation. For laser experiments, liquid solutions of the dyes were contained in 1 cm optical-path quartz cells that were carefully sealed to avoid solvent evaporation during the experiments. Both the liquid-containing cells and the solid polymeric samples were transversely pumped at 532 nm with 5.5 mJ, 6 ns fwhm pulses from a frequency-doubled Q-switched Nd:YAG laser (Monocrom OPL-10) at a repetition rate of 10 Hz. Some samples were pumped at 30 Hz with 5.5 mJ, 10 ns fwhm pulses from a diode pumped, frequency doubled, Q-switched Nd:YAG laser (Monocrom HALAZEN 532-12). The parallelism of the sample faces was controlled by illuminating the samples with the beam of a He-Ne laser along the axis of the cylinder and checking out the overlap of the reflections from both faces. Details of the experimental systems can be found elsewhere.^{11c}

We obtained narrow-line-width laser emission and tuning ranges of liquid solutions of the dyes by placing the samples in a homemade Shoshan-type oscillator^{11c} consisting of full-reflecting aluminum back and tuning mirrors and a 2400 lines mm^{-1} holographic grating in grazing incidence with outcoupling via the grating zero order. Wavelength tuning was accomplished by rotation of the tuning mirror. Tuning mirror and grating (both from Optometrics) were 5 cm wide, and the angle of incidence on the grating was 88.5° . Laser line width was measured with a Fabry–Perot etalon (IC Optical Systems) with a free spectral range of 15.9 GHz.

3. Results and Discussion

3.1. Synthesis. The dye PTA_r was synthesized in two steps (Scheme 1): (1) The reaction of 3-*tert*-butyl-2,4-dimethylpyrrole (**1**)¹⁵ with *p*-chloromethylbenzoyl chloride (**2**) yielded a substituted dipyrromethene that, after reacting in situ with boron trifluoride diethyl etherate in the presence of triethylamine, under conditions formerly used for the synthesis of similar dyes^{11d} produced the corresponding 8-*p*-chloromethylphenyl-BDP dye **3**. (2) Intermediate **3** was converted to PTA_r by reaction with sodium acetate in dimethylformamide (DMF).^{11d} PTA_rMA was similarly synthesized by the reaction of intermediate **3** with methacrylic acid in the presence of potassium carbonate in DMF. PTA_lk was obtained from the corresponding dipyrromethene (synthesized from **1** and 2-acetoxyacetyl-4-*tert*-butyl-3,5-dimethylpyrrole (**4**)), as before. PTH8 was isolated in the same reaction, although with very low yield (2%). The alternative synthesis of PTA_lk by the reaction between **1** and acetoxyacetyl chloride in toluene, under the conditions used for the synthesis of **3**, gave rise to PTH8 with higher yield (14%), although only traces (ca. 1%) of PTA_lk were detected. For more details of these syntheses, see the Supporting Information.

3.2. Photophysical Properties. The fluorescence bands of PTA_r, PTA_lk, and PM597 are broad (Figure 3), whereas PTH8 shows a band with the typical vibrational structure of most BDP dyes. The structureless emission bands can be ascribed to geometrical changes of the indacene core, mainly in the S_1 state.¹² Fluorescence decay curves of all of these analogues are monoexponential, with lifetimes in the range of 1.09–5.58 ns (Table 1). In PM597, quantum mechanical calculations indicate that the presence of the bulky *tert*-butyl groups at positions two and six induces a loss of planarity of the indacene core, with dihedral angles of the pyrrole units of ca. 3° in the S_0 state¹² (Figure 4, see also Table S1 in the Supporting Information). The loss of planarity is even more important in the S_1 state, with a dihedral angle of ca. 10° , explaining the important Stokes shift experimentally observed for this dye (ca. 1400 cm^{-1}).^{12,16} Quantum mechanical calculations at the DFT level for these analogues suggest that the disruption from the planarity of the pyrrole rings depends on the eight substituent. Indeed, a similar distorted geometry is theoretically obtained for PTA_r and PTA_lk, whereas a nearly planar structure is predicted for PTH8, without eight substituent, with a dihedral angle of the pyrrole rings of ca. 0.5° in its S_0 state and totally planar in the S_1 state (Figure 4). The S_1 planar structure of PTH8 leads to the observed fluorescence band with vibrational structure and with a short Stokes shift (190 cm^{-1}), a value much lower than the shift observed in the parent dye PM597.

In PTA_r, the deviation from the planarity in the S_0 state (dihedral angle of ca. 7°) is larger than that deduced for PM597 because of the additional steric hindrance between the *p*-phenylene ring at position eight and the methyl groups at positions one and seven. Indeed, and because of these methyl

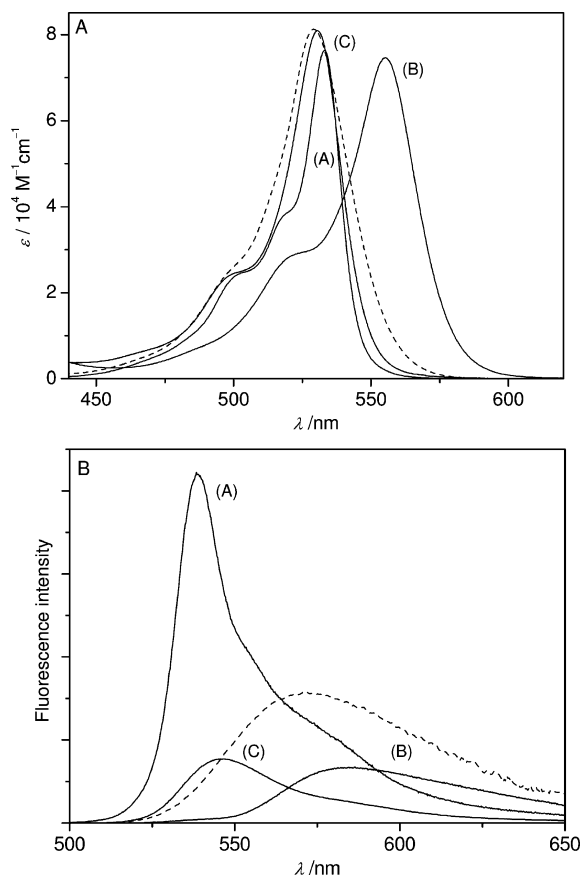


Figure 3. (A) Absorption and (B) fluorescence (normalized to their fluorescence quantum yield values) spectra of (A) PTH8, (B) PTA_lk, (C) PTA_r, and the parent dye PM597 (dashed line). 2×10^{-6} M solutions in cyclohexane.

TABLE 1: Photophysical Properties of PTA_r, PTH8, and PTA_lk and of the Parent Dye PM597, all 2×10^{-6} M in Cyclohexane, and Predicted Properties in Gas Phase^a

	data	PTA _r	PTH8	PTA _l k	PM597
experimental	$\lambda_{\text{abs}} (\pm 0.1)/\text{nm}$	530.5	533.0	555.0	529.0
	$\epsilon_{\text{max}} (\pm 0.1)/10^4\text{ M}^{-1}\text{ cm}^{-1}$	8.2	7.6	7.5	8.1
	$f (\pm 0.01)$	0.51	0.43	0.50	0.53
	$\lambda_{\text{flu}} (\pm 0.2)/\text{nm}$	547.5	538.5	586.5	571.0
	$\Delta\nu_{\text{St}}/\text{cm}^{-1}$	580	190	960	1395
	$\Phi_{\text{F}} (\pm 0.03)$	0.16	0.86	0.16	0.32
	$\tau (\pm 0.05)/\text{ns}$	1.32	5.58	1.09	3.91
	$k_{\text{fl}}/10^8\text{ s}^{-1}$	1.21	1.54	1.46	0.81
	$k_{\text{nr}}/10^8\text{ s}^{-1}$	6.36	0.25	7.70	1.74
predicted	$\Delta E_{\text{abs}}/\text{eV}$	2.86	2.89	2.71	2.89
	f	0.46	0.51	0.46	0.52
	$\Delta E_{\text{fl}}/\text{eV}$		2.88		2.72
	$k_{\text{fl}}/10^8\text{ s}^{-1}$		1.82		1.61

^a Absorption (λ_{abs}) and fluorescence (λ_{fl}) wavelength maxima, molar absorption coefficient (ϵ_{max}), oscillator strength (f), Stokes shift (ν_{St}), fluorescence quantum yield (Φ_{F}), lifetime (τ), radiative (k_{fl}), and nonradiative (k_{nr}) deactivation rate constants and energy gaps (ΔE_{abs} and ΔE_{fl}).

groups, quantum mechanical calculations suggest that the *p*-phenylene ring is twisted ca. 77° with respect to the indacene core. Such a disposition minimizes the overlap between the electronic π -clouds of both aromatic systems, avoiding the formation of new absorption and fluorescence bands. It is likely that the excitation of this distorted geometry does not modify the geometry of the indacene core, explaining the relatively low Stokes shift that is experimentally observed for PTA_r (580

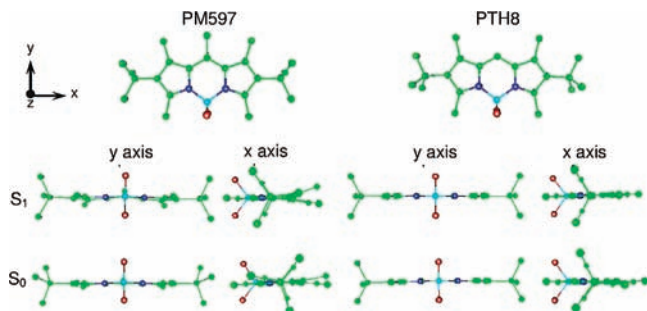


Figure 4. Theoretically optimized ground (S_0) and excited (S_1) state geometry of PM597 and PTH8.

cm^{-1}). PTalk, with an 8-acetoxymethyl group, shows an intermediate behavior with a moderate Stokes shift (ca. 960 cm^{-1}).

In PTalk, the 8-acetoxymethyl group induces a bathochromic shift of the absorption and fluorescence bands with respect to PM597 (Figure 3). Similar results were previously observed for related eight-substituted analogues of PM567,^{11b} and they can be ascribed to the electron-withdrawing effect of the acetoxymethyl group that stabilizes the high electronic density at position eight of the LUMO state with respect to the HOMO state.^{11b} When the acetoxymethyl group is separated from the indacene core by a *p*-phenylene group, as in PTAr, this electron-withdrawing effect is drastically reduced,¹⁷ and, consequently, only minimum spectral shifts, with respect to PM597, are observed in this dye (Figure 3). In this case, and as mentioned above, the phenylene ring is disposed nearly perpendicular to the indacene core, avoiding the overlapping of their respective electronic clouds.¹⁷

The fluorescence quantum yield and lifetime also show a marked change with the eight substituent (Table 1). Indeed, PTAr and PTalk present lower fluorescence quantum yields and lifetimes than their parent dye PM597, mainly because of an increase in the nonradiative deactivation rate constant. The opposite behavior is observed for PTH8 with much higher values for the fluorescence quantum yield and the lifetime. In previous work on the dye PM567 and its analogues,^{11b,d} it was observed that the inclusion of 8-acetoxymethyl or 8-*p*-acetoxymethylphenyl groups induce a decrease in the fluorescence quantum yield. In the case of the 8-acetoxymethyl analogue, this behavior was ascribed mainly to a decrease in the radiative rate constant due to the electron-withdrawing effect of the acetoxy group together with an increase in the nonradiative rate constant. In the case of the 8-*p*-acetoxymethylphenyl analogue, the observed increase in the internal conversion processes could be explained as the result of rotation/vibration of the pendant *p*-phenylene group. Similar explanations can be applied to the PM597 analogues. In the case of PTH8, the high fluorescence quantum yield (0.86, Table 1) and lifetime (5.58 ns) values are typical for most BDP dyes and can also be explained in terms of geometrical parameters. The absence of any substituent at the eight position in PTH8 drastically reduces the effect of the *tert*-butyl groups at the two and six positions on the planarity of the indacene core, favoring the radiative deactivation and reducing the internal conversion processes.

The solvent effect on the photophysical properties of the PM597 analogues (Supporting Information) is typical for most BDP dyes: spectral shifts (ca. 5 nm) to lower energies in polar/protic media and a low influence of the medium on the fluorescence quantum yield and Stokes shift. Taking into account the fact that the photophysics of the new analogues in polar

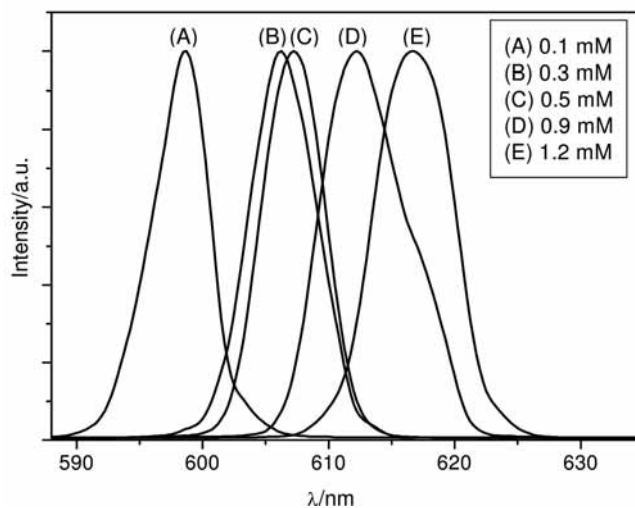
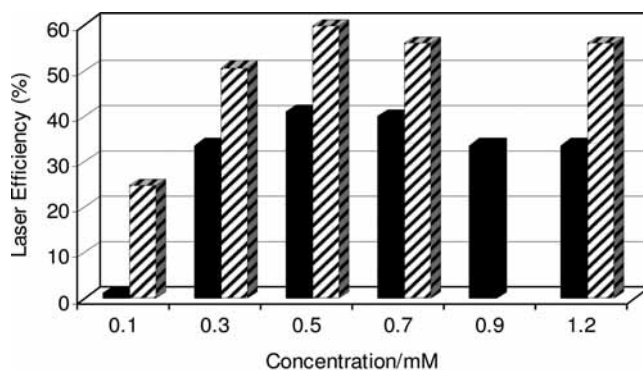


Figure 5. Lasing efficiencies in ethanol of PTalk (black bars) and PTAr (ray bars) (upper figure) and laser emission spectra of PTalk in ethanol as a function of the dye concentration.

protic solvents (methanol) is similar to that exhibited in the nonpolar solvent cyclohexane, it is difficult to choose the best media for achieving high lasing efficiencies.

3.3. Lasing Properties. 3.3.1. In Liquid Phase. The dependence of the laser action of each PM597 analogue on the dye concentration was analyzed in ethanol solutions with optical densities (1 cm path length) in the range of 1.5–35.0 while keeping constant all other experimental parameters. To assess the effect of the eight substituent on the laser operation, the lasing properties of solutions of PM597 were similarly studied. As an example, the lasing efficiencies and peak wavelengths of the emission of PTAr and PTalk as a function of the dye concentration are shown in Figure 5. As expected, the lasing efficiency of all analyzed solutions increased significantly with the dye concentration, reaching a maximum value for solutions with an optical density of ca. 15. The highest lasing efficiency was reached with the solutions with concentrations $5 \times 10^{-4} \text{ M}$ for PTAr and PTalk and $6 \times 10^{-4} \text{ M}$ for PTH8 and PM597. From this point on, further increases in dye concentration result in a decrease in lasing efficiency, with the laser emission being shifted to lower energies as the concentration increases. This dependence must be related to reabsorption/reemission phenomena on the laser emission intensity and could also be the origin of the decrease in the lasing efficiency observed in more concentrated solutions.¹⁸ Possible aggregation can be discarded because the shape of the absorption bands does not depend on the dye concentration.

The actual effect of the solvent in the dye lasing emission was analyzed in solutions with concentrations set at the values that optimize the lasing action in ethanol. In all selected solvents,

TABLE 2: Maximum Wavelength of the Laser Emission (λ_{laser}) and Energy Conversion Lasing Efficiency (eff) of the New Analogues of PM597 and of the Parent Dye PM597 in Several Solvents

dye	data	CF ₃ CH ₂ OH	MeOH	EtOH	acetone	ethyl acetate	cyclohexane
PTAr ^a	$\lambda_{\text{laser}}/\text{nm}$	560	561	561	562	562	565
	eff/%	50	52	60	50	55	35
PTH8 ^b	$\lambda_{\text{laser}}/\text{nm}$	561	560	562	561	560	563
	eff/%	50	60	58	61	63	59
PTAlk ^a	$\lambda_{\text{laser}}/\text{nm}$	612	609	607	608	608	615
	eff/%	42	45	40	51	52	44
PM597 ^b	$\lambda_{\text{laser}}/\text{nm}$	583	583	584	584	583	595
	eff/%	58	56	55	54	59	50

^a Dye concentration: 5×10^{-4} M. ^b Dye concentration: 6×10^{-4} M.

the dyes emit laser light with high efficiency (Table 2) similar to or even higher than that exhibited by the parent dye PM597 and other BDP dyes when pumped under identical experimental conditions,^{11a,b} with the lasing bands shifting toward lower energies as the solvent polarity decreases.

Good correlations between the photophysical properties (Table S2 in the Supporting Information) and the lasing characteristics (Table 2) of the new dyes can be observed. The maximum wavelengths of the lasing emissions and those of the fluorescence emissions follow the same solvent and eight-substituent dependence. In all of the selected solvents, the lowest fluorescence quantum yields were recorded for PTalk, which are related to a lower lasing efficiency of this dye. However, the low fluorescence quantum yield of PTalk could, to some extent, be compensated by its high Stokes shift, reducing the losses at the resonator cavity by reabsorption/reemission effects and giving rise to relatively high lasing efficiencies, similar to those registered for the other BDP analogues. PTH8 shows both the highest Φ_F and the lowest k_{nr} values (Table 1), which are nearly solvent independent, and, consequently, exhibits some of the highest lasing efficiencies (Table 2). In addition, the lasing efficiencies of PM597 and its analogue PTAr in cyclohexane solution follow the same behavior as that exhibited by their photophysical parameters: this apolar solvent impairs the lasing efficiency, with respect to the values registered in polar nonprotic and polar protic solvents.

3.3.2. In Solid State. The experiments were carried out using samples with the dye concentration producing the highest lasing efficiency in ethanol solution: $(5 \text{ to } 6) \times 10^{-4}$ M, depending on the dye. MMA was chosen as the main monomeric component of the formulations because this ester mimics ethyl acetate, a solvent where all studied dyes give rise to high lasing efficiencies. First, the dyes were incorporated as true solutions into the solid homopolymer PMMA to establish the effect of the eight substituent on their lasing action when pumped under the experimental conditions described above. To put the present results into proper perspective, the lasing parameters of PM597 in PMMA were also measured under the same conditions (Table 3).

Broad-band and efficient laser emission, with beam divergence of ca. 5 mrad and pulse duration of ca. 5 ns fwhm, was registered from all the solid solutions. No significant differences were observed in the wavelength of the maximum laser emission of each dye between their liquid and solid solutions. The lasing efficiencies of the solid materials, in the range of 31–48%, are somewhat lower than those of the corresponding ethyl acetate solutions. In this regard, it has to be taken into account that the finishing of the surface of the solid samples relevant to the laser operation was not laser-grade so that even higher lasing efficiencies are to be expected with laser-grade surfaces.

TABLE 3: Laser Parameters of PM597 and Their Analogues Incorporated into PMMA, PHEMA, and into Copolymers of MMA with HEMA or TMSPPMA^{a,b}

dye	solid medium	eff/%	$\lambda_{\text{laser}}/\text{nm}$	I/%	tuning range/nm
PTAr	PMMA	46	559	63	540–580
PTArMA	PMMA	38	559	61	
PTH8	PMMA	48	562	85	540–585
	COP(MMA-HEMA 7:3)	47	565	88	
	COP(MMA-HEMA 5:5)	39	566	100	
	COP(MMA-HEMA 3:7)	35	567	65	
	PHEMA	31	568	37	
PTalk	PMMA	48	606	98	585–625
	COP(MMA-HEMA 7:3)	42	605	98	
	COP(MMA-HEMA 5:5)	40	606	70	
	COP(MMA-HEMA 3:7)	35	609	45	
	PHEMA	31	609	30	
	COP(MMA-TMSPPMA 9:1)	42	606	100	
	COP(MMA-TMSPPMA 7:3)	42	607	100	
PM597	PMMA	52	580	88	555–580

^a As defined in Table 2; *I*: intensity of the dye laser output after 100 000 pump pulses in the same position of the sample, referred to the initial intensity I_0 , $I = 100(I/I_0)$, at 10 Hz repetition rate and 5.5 mJ pulse⁻¹. ^b Same parameters for PTArMA covalently bound to PMMA are also included.

We studied the lasing stabilities of the dyes in PMMA solutions by following the evolution of the laser output as a function of the number of pump pulses in the same position of the sample at 10 Hz repetition rate. The photophysical data of the dyes in different solvents, commented above, provide useful information on the potential of the solid materials as laser media. Both the lasing efficiency and the photostability in solid solution are higher when the fluorescence quantum yield and the Stokes shift are higher and when the nonradiative rate constant is lower. Therefore, the shift to higher energies of the PTAr lasing band with respect to that of PM597 significantly reduces the Stokes shifts, increases the reabsorption/reemission effects, and drastically impairs the photostability.

Contrary to the behavior previously observed in other BDP dyes,^{11d} the covalent bonding of the monomeric dye PTArMA to PMMA chains does improve neither the lasing efficiency nor the photostability of the chromophore with respect to the model dye PTAr dissolved in PMMA. It is very likely that the extension and probability of the reabsorption/reemission effects are favored by the low Stokes shift and could counteract the improvement in the dissipation of the excess of absorbed energy not converted into emission, provided by the covalent linkage of the dye to the polymeric chain. According to this argument, a higher Stokes shift should result in a higher photostability, as is seen in the case of PTalk/PMMA if compared with PTAr/PMMA. Notwithstanding, PTH8, which in cyclohexane solution presents the lowest Stokes shift but the highest fluorescence quantum yield and the lowest nonradiative constant (Table 1), exhibits in PMMA a high photostability, reflecting the difficulty of understanding at the present time the detailed mechanism of the emission process of these dyes in the solid state.

To study the influence of the polymeric medium polarity on the laser action of the dyes, we also prepared solid solutions of the analogues PTH8 and PTalk in copolymers of MMA with different volumetric proportions of the more polar monomer HEMA (Table 3). It is seen that an increase in the polarity of the medium results in a slight hypsochromic shift of the laser emissions. Lasing efficiencies and photostabilities are similar or slightly lower than those obtained with the same dye dissolved in the homopolymer PMMA. High proportions of HEMA impair

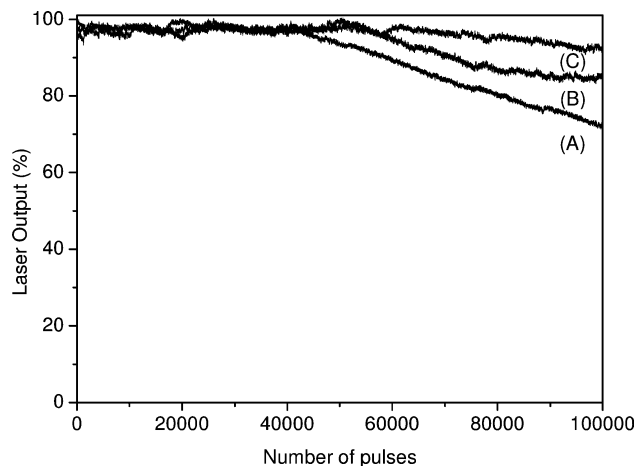


Figure 6. Normalized laser output as a function of the number of pump pulses at 30 Hz repetition rate in the same position of the sample for PTalk incorporated into (A) PMMA, (B) COP(MMA-TMSPMA 9:1), and (C) COP(MMA-TMSPMA 7:3).

the laser action of PTH8 and, more significantly, that of PTalk, following in some way the same dependence of the photophysical properties of these dyes on the liquid solvent polarity. Previous studies had revealed that the laser action of BDP dyes in polymeric matrices was greatly enhanced by properly incorporating monomers with silicon atoms in their structures.¹⁸ Therefore, trying to improve the laser action of the new dyes in polymeric solid materials further, PTalk, the dye with the highest photostability in pure PMMA, was incorporated as true solutions into copolymers of MMA with TMSPMA in volumetric proportions in the range of 10–30%. Taking into account the fact that TMSPMA has one silicon atom per mole, the concentration of silicon atoms in the solid copolymers varies from 1% in COP(MMA-TMSPMA 9:1) to 4% in COP(MMA-TMSPMA 7:3). The laser performance of PTalk in the silicon-containing organic matrices under 10 Hz pumping repetition rate was similar to that obtained in pure PMMA homopolymer.

The accumulation of heat into polymeric solid-state dye lasers increases significantly with the pumping repetition rate, resulting in a decrease in the lasing stability.¹⁹ Consequently, we proceeded to pump at a 30 Hz repetition rate some of the PTalk-doped solid materials that previously exhibited good photostability when pumped at 10 Hz (Figure 6). Under 30 Hz, PTalk showed a steady decrease in the laser output with the number of pump pulses, which is faster in the sample with lower silicon content. The best overall laser performance was obtained with PTalk incorporated as solid solution into COP(MMA-TMSPMA 7:3), where the lasing efficiency was 42% and the laser emission was highly stable, remaining at 90% of its initial laser output intensity after 100 000 pump pulses at a 30 Hz repetition rate in the same position of the sample. The lasing photostability increases with the content of the silicon-modified monomer in the matrix because of the improved thermal conductivity of the copolymers with respect to the homopolymer PMMA.¹⁹

To put the present results into proper perspective, the lasing parameters of PM567 and sulforhodamine B, two well-known dyes that lase at the same wavelengths as the herein studied dyes, were also measured in solid solutions under comparative conditions. PM567 in PMMA lased at 562 nm with an efficiency of 39% and with low photostability, with only 30% of its initial emission intensity remaining after 100 000 pump pulses at 10 Hz. Likewise, sulforhodamine B incorporated into the homopolymer PHEMA (the low solubility of this dye in PMMA precludes its incorporation into this polymer) lased at 604 nm

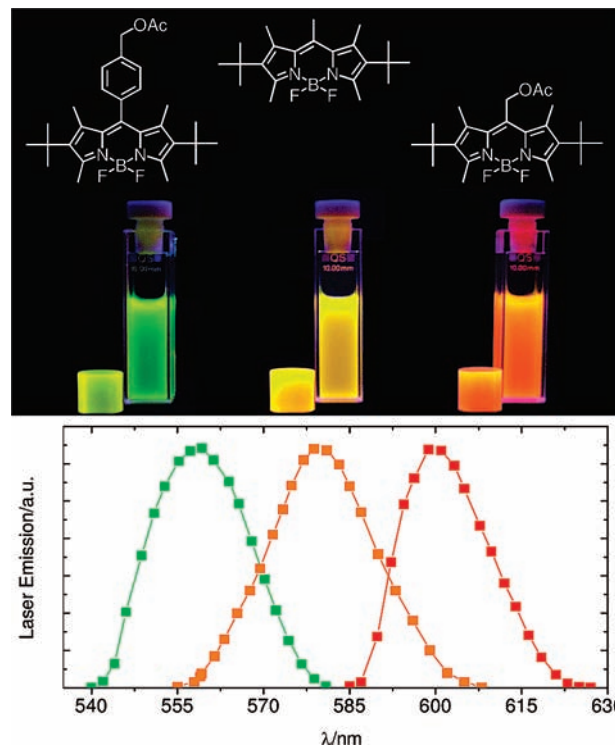


Figure 7. Modulated laser tunability of PTAr, PM597 and PTalk in ethanol. Similar results are reached in solid polymeric solutions.

with an efficiency of 32%, but the laser emission disappeared after just 70 000 pump pulses. Consequently, the new analogues of PM597 incorporated into polymeric matrices outperform the laser action of dyes considered to be benchmarks over the spectral region from the green-yellow to the red.

We determined the tuning capability of the new dyes, one of the most important features of laser dyes, by placing their solid and liquid solutions in a grazing-incidence grating tunable resonator. Tunable laser emission with line width on the order of 0.15 cm^{-1} and tuning range of up to 50 nm was recorded (Table 3, Figure 7), so that the spectral region 540–625 nm can be continuously covered with narrow-line-width and stable laser radiation by using these dyes.

4. Conclusions

We have designed and synthesized tailor-made BDP dyes for applications that require absorption and emission in specific regions of the visible near-IR spectral range. The new dyes are analogues of the commercial laser dye PM597 with 8-hydrogen (PTH8), 8-acetoxymethyl (PTalk), or 8-*p*-acetoxymethylphenyl (PTAr) groups instead of the 8-methyl group. The different eight-substituents allowed us to analyze the influence of the geometrical distortion of the indacene core, induced by the presence of the 2,6-di-*tert*-butyl and 1,7-dimethyl groups, on the corresponding photophysical and lasing properties.

In liquid solutions, the photophysical parameters depend on the nature of the solvent in the same way as that previously observed in other BDP dyes: hypsochromic shifts of the absorption and fluorescence bands in polar/protic media and a low dependence of the fluorescence quantum yield and Stokes shift on the polarity of the media. Good correlations between the photophysical properties of the new dyes in diluted solutions and the lasing characteristics in more concentrated solutions have been observed. The new BDP dyes show high lasing emission efficiencies that are similar to or even higher than those exhibited

by the parent dye PM597 under transversal pumping at 532 nm in a simple nonoptimized plane–plane laser cavity. In the liquid phase, the highest lasing efficiencies (60%) were registered with PTAr in ethanol and with the analogues PTH8 (63%) and PTalk (52%) in ethyl acetate. When the new dyes were dissolved in solid PMMA, lasing efficiencies of up to 48% were obtained. The highest lasing photostability corresponded to PTalk in the copolymeric matrix MMA-TMSPMA 7:3 v/v, where the laser emission was still 90% of its initial value after 100 000 pump pulses at 30 Hz in the same position of the sample.

The laser action of the new BDP dyes outperforms that of other laser dyes considered to be benchmarks over the green-yellow to red spectral region and, when incorporated into a wavelength-selective resonator, allowed the spectral region to be covered from 540 to 625 nm with continuous tunable narrow-line-width and stable laser radiation. Considering the easy synthetic buildup, the wide variety of possible substituents, and the large number of described BDP laser dyes, we are confident that this powerful approach could be extended to other dyes of this family with practical applications in optical and sensing fields.

Acknowledgment. This work was supported by projects MAT2007-65778-C02-01 and -02 of the Spanish Ministerio de Investigación, Ciencia e Innovación (MICIN). M.P.-S. thanks MICIN for a predoctoral scholarship (cofinanced by Fondo Social Europeo). M.L. was a recipient of a Juan de la Cierva contract (MICIN).

Supporting Information Available: Synthesis and characterization of compounds, dihedral angles of the optimized geometries of PTalk and PTAr, and photophysical properties of the studied dyes in liquid solution. This material is available free of charge via the Internet at <http://pubs.acs.org>.

References and Notes

- (1) Valeur, B. *In Molecular Fluorescence: Principles and Applications*; Wiley-VCH: Weinheim, Germany, 2002.
- (2) Lakowicz, J. R. *Probe Design and Chemical Sensing. In Topics in Fluorescence Spectroscopy*; Plenum: New York, 1994; Vol. 4.
- (3) Loudet, A.; Burgess, K. *Chem. Rev.* **2007**, *107*, 4891.
- (4) Haugland, R. P. *The Handbook: A Guide to Fluorescent Probes and Labelling Technologies*; Spence, M. T. Z., Ed.; Molecular Probes: Eugene, OR, 2005.
- (5) (a) Burghart, A.; Kim, H.; Welch, M. B.; Thoresen, L. H.; Reibenspies, J.; Burgess, K. *J. Org. Chem.* **1999**, *64*, 7813. (b) Chen, J.; Burghart, A.; Derecskei-Kovacs, A.; Burgess, K. *J. Org. Chem.* **2000**, *65*, 2900. (c) Turfan, B.; Akkaya, E. U. *Org. Lett.* **2002**, *4*, 2857. (d) Coskun, A.; Akkaya, E. U. *J. Am. Chem. Soc.* **2005**, *127*, 10464. (e) Quin, W.; Rohand, T.; Baruah, M.; Stefan, A.; Van der Auweraer, M.; Dehaen, W.; Boens, N. *Chem. Phys. Lett.* **2006**, *420*, 562. (f) For a recent review, see: Descalzo, A. B.; Xu, H. J.; Shen, Z.; Rurack, K. *Ann. N.Y. Acad. Sci.* **2008**, *1130*, 164.
- (6) (a) Burghart, A.; Thoresen, L. H.; Chen, J.; Burgess, K.; Bergström, F.; Johansson, L. B. A. *Chem. Commun.* **2000**, *22*, 2203. (b) Maas, H.; Calzaferri, G. *Angew. Chem., Int. Ed.* **2002**, *41*, 2284. (c) Ulrich, G.; Goze, C.; Guardigli, C. M.; Roda, A.; Ziessel, R. *Angew. Chem., Int. Ed.* **2005**, *44*, 3694.
- (7) (a) Rurack, K.; Kollmannsberger, M.; Resch-Genger, U.; Daub, J. *J. Am. Chem. Soc.* **2000**, *122*, 968. (b) Turfan, B.; Akkaya, E. U. *Org. Lett.*

2002, *4*, 2857. (c) Ulrich, G.; Ziessel, R. *J. Org. Chem.* **2004**, *69*, 2070. (d) Gabe, Y.; Urano, Y.; Kikuchi, K.; Kojima, H.; Nagano, T. *J. Am. Chem. Soc.* **2004**, *126*, 3357. (e) Basaric, N.; Baruah, M.; Quin, W.; Metten, B.; Smet, M.; Dehaen, W.; Boens, N. *Org. Biomol. Chem.* **2005**, *3*, 2755. (f) Zeng, L.; Miller, E. W.; Pralle, A.; Isacoff, E. Y.; Chang, C. J. *J. Am. Chem. Soc.* **2006**, *128*, 10.

(8) (a) Tan, K.; Jaquinod, L.; Paolesse, R.; Nardis, S.; Di Natale, C. D.; Di Carlo, A.; Prodi, L.; Montalti, M.; Zaccaroni, N.; Nith, K. M. *Tetrahedron* **2004**, *60*, 1099. (b) Yee, M.; Fas, S. C.; Stohlmeyer, M. M.; Wandless, T. J.; Cimprich, K. A. *J. Biol. Chem.* **2005**, *280*, 29053.

(9) *Fluorescence Spectroscopy in Biology: Advanced Methods and Their Applications to Membranes Proteins, DNA, and Cells*; Martin, H., Rudolf, H., Vlastimil, F., Eds.; Springer-Verlag: Heidelberg, Germany, 2005.

(10) (a) Assor, Y.; Burshtein, Z.; Rosenwaks, S. *Appl. Opt.* **1988**, *37*, 4914. (b) Pavlopoulos, T. G.; Sha, M.; Boyer, J. H. *Opt. Commun.* **1989**, *70*, 425. (c) Guggenheimer, S. C.; Boyer, J. H.; Thangaraj, K.; Soong, M.-L.; Pavlopoulos, T. G. *Appl. Opt.* **1993**, *32*, 3942. (d) O'Neil, M. P. *Opt. Lett.* **1993**, *18*, 37. (e) Partridge, W. D., Jr.; Laurendeau, N. M.; Johnson, C. C.; Steppel, R. N. *Opt. Lett.* **1994**, *19*, 1639.

(11) (a) Costela, A.; García-Moreno, I.; Gómez, C.; Amat-Guerri, F.; Sastre, R. *Appl. Phys. Lett.* **2001**, *79*, 305. (b) Costela, A.; García-Moreno, I.; Gómez, C.; Sastre, R.; Amat-Guerri, F.; Liras, M.; López Arbeloa, F.; Bañuelos Prieto, J.; López Arbeloa, I. *J. Phys. Chem. A* **2002**, *106*, 7736. (c) Costela, A.; García-Moreno, I.; Sastre, R. *Phys. Chem. Chem. Phys.* **2003**, *5*, 4745. (d) García-Moreno, I.; Costela, A.; Campo, L.; Sastre, R.; Amat-Guerri, F.; Liras, M.; López Arbeloa, F.; Bañuelos Prieto, J.; López Arbeloa, I. *J. Phys. Chem. A* **2004**, *108*, 3315. (e) Álvarez, M.; Amat-Guerri, F.; Costela, A.; García-Moreno, I.; Gómez, C.; Liras, M.; Sastre, R. *Appl. Phys. B: Laser Opt.* **2005**, *80*, 993. (f) Álvarez, M.; Costela, A.; García-Moreno, I.; Amat-Guerri, F.; Liras, M.; Sastre, R.; López Arbeloa, F.; Bañuelos Prieto, J.; López Arbeloa, I. *Photochem. Photobiol. Sci.* **2008**, *7*, 802.

(12) Bañuelos Prieto, J.; López Arbeloa, F.; Martínez Martínez, V.; Arbeloa López, T.; López Arbeloa, I. *J. Phys. Chem. A* **2004**, *108*, 5503.

(13) (a) Nung, T. H.; Canva, M.; Dao, T. T. A.; Chaput, F.; Brun, A.; Hung, N. D.; Boicot, J. P. *Appl. Opt.* **2003**, *42*, 2213. (b) Reisfeld, R.; Weiss, A.; Saraidarov, T.; Yariv, E.; Ishchenko, A. A. *Polym. Adv. Technol.* **2004**, *15*, 291. (c) Costela, A.; García-Moreno, I.; Del Agua, D.; García, O.; Sastre, R. *J. Appl. Phys.* **2007**, *101*, 73110.

(14) Frisch, M. J.; Trucks, G. W.; Schlegel, H. B.; Scuseria, G. E.; Robb, M. A.; Cheeseman, J. R.; Montgomery, J. A., Jr.; Vreven, T.; Kudin, K. N.; Burant, J. C.; Millam, J. M.; Iyengar, S. S.; Tomasi, J.; Barone, V.; Mennucci, B.; Cossi, M.; Scalmani, G.; Rega, N.; Petersson, G. A.; Nakatsuji, H.; Hada, M.; Ehara, M.; Toyota, K.; Fukuda, R.; Hasegawa, J.; Ishida, M.; Nakajima, T.; Honda, Y.; Kitao, O.; Nakai, H.; Klene, M.; Li, X.; Knox, J. E.; Hratchian, H. P.; Cross, J. B.; Bakken, V.; Adamo, C.; Jaramillo, J.; Gomperts, R.; Stratmann, R. E.; Yazyev, O.; Austin, A. J.; Cammi, R.; Pomelli, C.; Ochterski, J. W.; Ayala, P. Y.; Morokuma, K.; Voth, G. A.; Salvador, P.; Dannenberg, J. J.; Zakrzewski, V. G.; Dapprich, S.; Daniels, A. D.; Strain, M. C.; Farkas, O.; Malick, D. K.; Rabuck, A. D.; Raghavachari, K.; Foresman, J. B.; Ortiz, J. V.; Cui, Q.; Baboul, A. G.; Clifford, S.; Cioslowski, J.; Stefanov, B. B.; Liu, G.; Liashenko, A.; Piskorz, P.; Komaromi, I.; Martin, R. L.; Fox, D. J.; Keith, T.; Al-Laham, M. A.; Peng, C. Y.; Nanayakkara, A.; Challacombe, M.; Gill, P. M. W.; Johnson, B.; Chen, W.; Wong, M. W.; Gonzalez, C.; Pople, J. A. *Gaussian 03*; Gaussian, Inc.: Wallingford, CT, 2004.

(15) (a) Treibs, A.; Schulze, L. *Liebigs Ann. Chem.* **1970**, *739*, 222. (b) Treibs, A.; Schulze, L. *Liebigs Ann. Chem.* **1970**, *739*, 225.

(16) Lai, R. Y.; Bard, A. J. *J. Phys. Chem. B* **2003**, *107*, 5036.

(17) Bañuelos Prieto, J.; López Arbeloa, F.; Martínez Martínez, V.; Arbeloa López, T.; Amat-Guerri, F.; Liras, M.; López Arbeloa, I. *Chem. Phys. Lett.* **2004**, *385*, 29.

(18) López Arbeloa, I. *J. Photochem.* **1980**, *14*, 97.

(19) (a) Costela, A.; García-Moreno, I.; Del Agua, D.; García, O.; Sastre, R. *Appl. Phys. Lett.* **2004**, *85*, 2160. (b) Costela, A.; García-Moreno, I.; Del Agua, D.; García, O.; Sastre, R. *J. Appl. Phys.* **2007**, *101*, 073110.

(20) Duchowicz, R.; Scaffardi, L. B.; Costela, A.; García-Moreno, I.; Sastre, R.; Acuña, A. U. *Appl. Opt.* **2003**, *42*, 1029.

JP902734M